Chapter 5

Loop Antennas

Glenn S. Smith

Georgia Institute of Technology

CONTENTS

5.1 INTRODUCTION 5-2

5.2 ELECTRICALLY SMALL LOOPS 5-2

5.3 ELECTRICALLY LARGE LOOPS 5-9

5.4 SHIELDED-LOOP ANTENNA 5-18

5.5 PULSE-EXCITED CIRCULAR-LOOP ANTENNA 5-20

5.6 ADDITIONAL TOPICS 5-22

5.1 INTRODUCTION

The single-turn loop antenna is a metallic conductor bent into the shape of a closed curve, such as a circle or a square, with a gap in the conductor to form the terminals. A multiturn loop or coil is a series connection of overlaying turns. The loop is one of the primary antenna structures; its use as a receiving antenna dates back to the early experiments of Hertz on the propagation of electromagnetic waves.[1]

The discussion of loop antennas is conveniently divided according to electrical size. Electrically small loops, those whose total conductor length is small compared with the wavelength in free space, are the most frequently encountered in practice. For example, they are commonly used as receiving antennas with portable radios, as directional antennas for radio-wave navigation, and as probes with field-strength meters. Electrically larger loops, particularly those near resonant size (circumference of loop/wavelength ≈ 1), are used mainly as elements in directional arrays.

The following symbols are used throughout the chapter:

λ = wavelength in free space at the frequency $f = \omega/2\pi$, when the complex harmonic time-dependence exp ($j\omega t$) is assumed
$\beta = 2\pi/\lambda$ = propagation constant in free space
$\zeta = \sqrt{\mu_0 / \varepsilon_0}$ = wave impedance of free space (≈ 377 Ω)
b = mean radius of a circular loop or mean side length of a square loop
a = radius of loop conductor (All results presented are for thin-wire loops, $a/b \ll 1$.)
A = area of loop
N = number of turns
ℓ_c = length of solenoidal coil

5.2 ELECTRICALLY SMALL LOOPS

The axial current distribution in an electrically small loop is assumed to be uniform; that is, the current has the same value I_0 at any point along the conductor. For single-turn loops and multiturn loops that are single-layer solenoidal coils, measurements suggest that this is a good assumption provided the total length of the conductor ($N \times$ circumference) is small compared with the wavelength in free space, typically $\leq 0.1\lambda$, and the length-to-diameter ratio for the solenoidal coil is greater than about 3 ($\ell_c/2b \geq 3.0$).[2] With a uniform current assumed, the electrically small loop antenna is simply analyzed as a radiating inductor.[3]

Transmitting Loop

The electromagnetic field of an electrically small loop antenna is the same as that of a magnetic dipole with moment $m = I_0 NA$:

$$E_\phi = \frac{\zeta \beta^2 m}{4\pi r}\left(1 - \frac{j}{\beta r}\right) e^{-j\beta r} \sin\theta \tag{5-1}$$

$$B_\theta = \frac{-\mu_0 \beta^2 m}{4\pi r}\left(1 - \frac{j}{\beta r} - \frac{1}{\beta^2 r^2}\right) e^{-j\beta r} \sin\theta \tag{5-2}$$

$$B_r = \frac{\mu_0 \beta^2 m}{2\pi r}\left(\frac{j}{\beta r} + \frac{1}{\beta^2 r^2}\right) e^{-j\beta r} \cos\theta \tag{5-3}$$

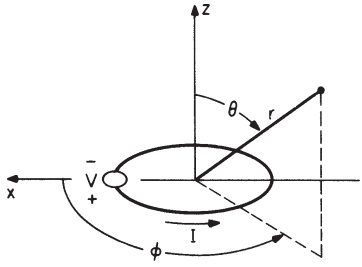

FIGURE 5-1 Loop antenna and accompanying spherical coordinate system

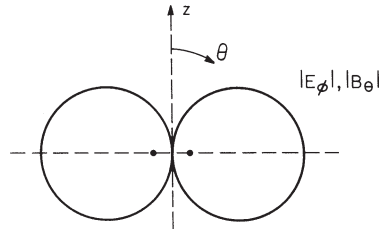

FIGURE 5-2 Far-zone vertical-plane field pattern of an electrically small loop

in which the plane of the loop is normal to the polar axis of the spherical coordinate system (r, θ, ϕ) centered at the loop, as shown in Figure 5-1. In the far zone of the loop ($\lim \beta r \to \infty$), only the leading terms in Eqs. 5-1 and 5-2 are significant, and the field pattern for both E_ϕ and B_θ in the vertical plane is the simple figure eight shown in Figure 5-2.

The driving-point voltage and current are related through the input impedance of the loop, $V = ZI_0$. For electrically small loops, the impedance is the series combination of the reactance of the external inductance L^e with the radiation resistance R^r and the internal impedance of the conductor $Z^i = R^i + j\omega L^i$:

$$Z = R + j\omega L = R^r + Z^i + j\omega L^e = R^r + R^i + j\omega(L^e + L^i) \tag{5-4}$$

The internal resistance R^i accounts for ohmic loss. In the equivalent circuit for the small loop, a lumped capacitance C is sometimes placed in parallel with Z to account for the distributed capacitance between the sides of a single turn and between the turns of a solenoid, as shown in Figure 5-3. Note that a loop with a truly uniform current distribution would have no capacitance, since from the equation of continuity there would be no charge along the conductor of the loop.

The radiation resistance of the small loop is proportional to the square of the product of the area and the number of turns:

$$R^r = \frac{\zeta}{6\pi}\beta^4 (NA)^2 \tag{5-5}$$

For single-turn loops and solenoidal coils whose turns are not too closely spaced, the internal impedance is approximately

$$Z^i = z^i \times \text{total length of conductor} \tag{5-6}$$

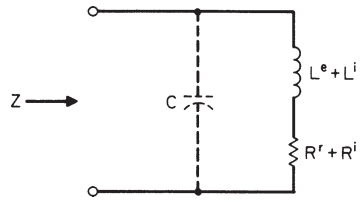

FIGURE 5-3 Equivalent circuit for input impedance Z of an electrically small loop

in which z^i is the internal impedance per unit length of a straight conductor with the same cross section as the loop conductor.[4] If the turns of the coil are closely spaced, the proximity effect must also be included in determining Z^i.[5]

The external inductance is determined from one of the many formulas available for the inductance of coils:[6] For a single-turn circular loop

$$L^e = \mu_0 b[\ln (8b/a) - 2] \tag{5-7}$$

and for a single-turn square loop

$$L^e = \frac{2\mu_0 b}{\pi}[\ln (b/a) - 0.774] \tag{5-8}$$

The external inductance of a tightly wound single-layer solenoidal coil of N turns, length ℓ_c, and radius b is often approximated by Lorenz's formula for the inductance of a circumferentially directed current sheet.[6] Numerical results from this formula can be put in a form convenient for application:

$$L^e = K\mu_0 N^2 A/\ell_c \tag{5-9}$$

in which the factor K, known as Nagaoka's constant, is shown as a function of the ratio $\ell_c/2b$ (length of the coil to the diameter) in Figure 5-4. Note that, for a long coil ($\ell_c/2b \gg 1$), $K \approx 1$. The use of Eq. 5-9 assumes that the turns of the coil are so closely spaced that the winding pitch and insulation on the conductors can be ignored; if highly accurate calculations of L^e are necessary, corrections for these factors are available in the literature.[6]

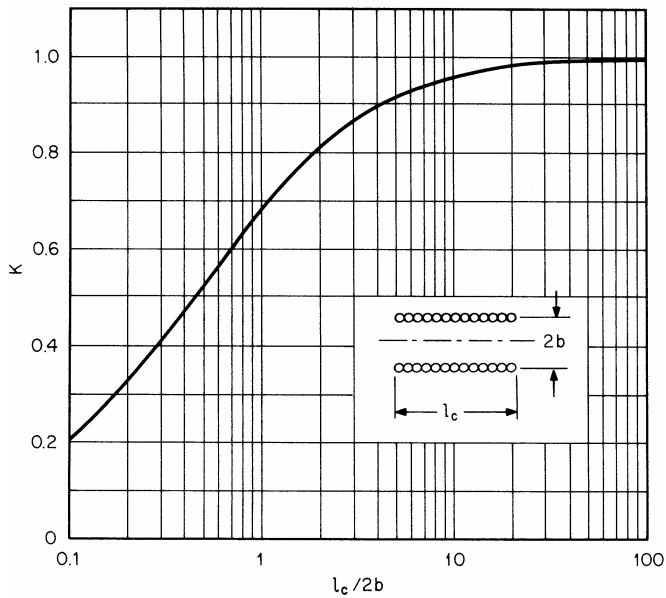

FIGURE 5-4 Nagaoka's constant K for a solenoidal coil as a function of the coil length to the diameter, $\ell_c/2b$

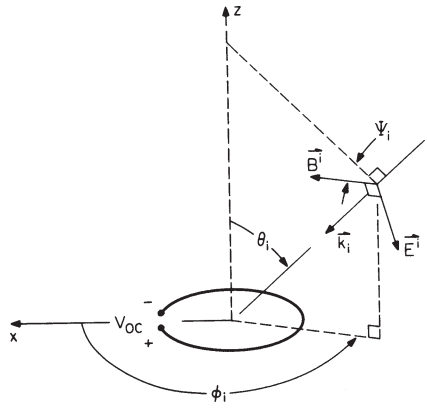

FIGURE 5-5 Plane-wave field incident on receiving loop

The radiation efficiency of the electrically small transmitting loop antenna is

$$\eta = \frac{\text{Time-Average Power Radiated}}{\text{Time-Average Power Supplied}} = \frac{R^r}{R^r + R^i} \tag{5-10}$$

The ohmic resistance R^i is often comparable to or larger than the radiation resistance R^r, so the radiation efficiency can be low.[5] It can be increased by decreasing the ohmic resistance of the loop, i.e., by using a conductor of lower resistivity or larger radius.

Receiving Loop

When the electrically small loop is used as a receiving antenna, the voltage developed at its open-circuited terminals V_{OC} is proportional to the component of the incident magnetic flux density normal to the plane of the loop B_z^i:

$$V_{OC} = j\omega NAB_z^i \tag{5-11}$$

in which the incident field is assumed to be uniform over the area of the loop. This simple relation between V_{OC} and B_z^i makes the small loop useful as a probe for measuring the magnetic flux density. If a relation between the incident electric and magnetic fields at the center of the loop is known, V_{OC} can be expressed in terms of the magnitude of the incident electric field E^i and an effective height h_e. This is the case for an incident linearly polarized plane wave with the wave vector $\mathbf{k}_i$ and the orientation shown in Figure 5-5:

$$V_{OC} = j\omega\, NAB^i \cos\,\psi_i \sin\,\theta_i = h_e(\psi_i, \theta_i)E^i \tag{5-12}$$

in which

$$h_e(\psi_i, \theta_i) \equiv V_{OC}/E^i = j\beta NA \cos\,\psi_i \sin\,\theta_i \tag{5-13}$$

The voltage across an arbitrary load impedance Z_L connected to the terminals of the loop with input impedance Z is determined from the Thévenin equivalent circuit in Figure 5-6:

$$V_L = V_O\, Z_L/(Z + Z_L) \tag{5-14}$$

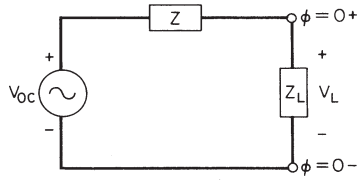

FIGURE 5-6 Thévenin equivalent circuit for the receiving loop

Ferrite-Loaded Receiving Loop

The open-circuit voltage at the terminals of the electrically small receiving loop can be increased by filling the loop with a core of permeable material, usually a ferrite. The effect of the core is to increase the magnetic flux through the area of the loop, as illustrated in Figure 5-7 for a solenoidal coil with a cylindrical core placed in a uniform axial magnetic field.

The ferrite material is characterized by a complex relative initial permeability $\mu_r = \mu/\mu_0 = \mu_r' - j\mu_r''$ and a relative permittivity $\varepsilon_r = \varepsilon/\varepsilon_0$.* The material is usually selected to have a loss tangent $p_m = \mu_r''/\mu_r'$ that is small at the frequency of operation. Consequently, μ_r'' is ignored in the analysis except when the power dissipated in the core is being calculated. The dimensions of the core are also assumed to be small compared with the wavelength in the ferrite $\lambda_m \approx \lambda/\sqrt{\varepsilon_r \mu_r'}$ to prevent internal resonances within the core.[7]

The open-circuit voltage for a single-turn loop at the middle of a ferrite cylinder of length ℓ_r and radius b is increased by the factor μ_{rod} over the value for the same loop in free space:

$$V_{\text{OC}} = j\omega\mu_{\text{rod}} A B_z^i \tag{5-15}$$

Here the radius of the loop conductor a is ignored, and the mean radius of the loop and the core are assumed to be the same value b. The graph in Figure 5-8 shows the apparent permeability μ_{rod} as a function of the length-to-diameter ratio for the rod $\ell_r/2b$ with the relative initial permeability of the ferrite μ_r' as a parameter.[8] Similar graphs for the apparent permeability of solid and hollow spheroidal cores are in the literature.[9]

For a single-layer solenoidal coil of length ℓ_c centered on the rod, an averaging factor F_V must be included in the open-circuit voltage to account for the decrease in the flux along the length of the coil from the maximum at the middle:

$$V_{\text{OC}} = j\omega\mu_{\text{rod}} F_V N A B_z^i \tag{5-16}$$

The empirical factor F_V, determined from an average of experimental results, is shown in Figure 5-9 as a function of the ratio ℓ_c/ℓ_r (length of the coil to length of the rod).[10,11] For a long rod of moderate permeability ($\ell_r/2b \gg 1$, $\mu_{\text{rod}} \approx \mu_r'$) covered by a coil of equal length ($\ell_c/\ell_r = 1$), the open-circuit voltage is increased by approximately the factor 0.8 μ_r' over the open-circuit voltage for the same coil without the core.

The equivalent circuit for the impedance of the ferrite-loaded solenoidal coil is that shown in Figure 5-3 with an additional series resistor R^m included to account for the power dissipated in the core. The elements in the circuit are the radiation resistance:

$$R^r = \frac{\zeta}{6\pi}\beta^4(\mu_{\text{rod}} F_V N A)^2 \tag{5-17}$$

*The initial permeability is the derivative dB/dH in the limit as H is reduced to zero. Dielectric loss in the ferrite is ignored here, and the permittivity is assumed to be real.

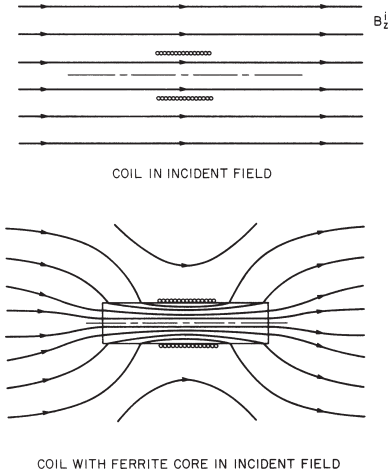

FIGURE 5-7 Effect of a cylindrical ferrite core on the magnetic flux through a solenoidal coil

the resistance due to core loss:

$$R^m = \omega(\mu_{\text{rod}}/\mu_r')^2 \mu_r'' \mu_0 F_R N^2 A/\ell_c \tag{5-18}$$

and the external inductance of the loaded solenoidal coil:

$$L^e = \mu_{\text{rod}} F_L \mu_0 N^2 A/\ell_c \tag{5-19}$$

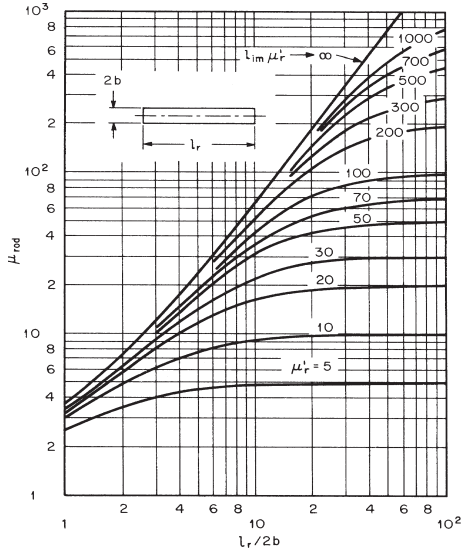

FIGURE 5-8 The apparent permeability μ_{rod} at the middle of a cylindrical rod as a function of the length-to-diameter ratio $\ell_r/2b$ with the initial permeability μ_r' as a parameter

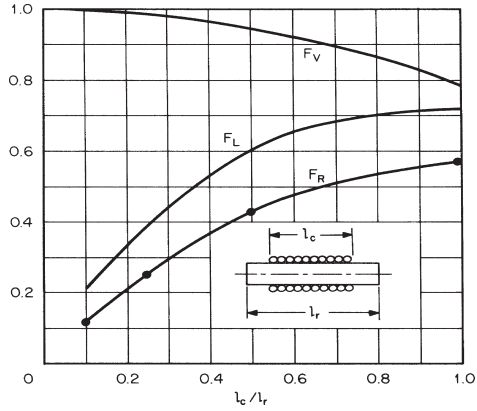

FIGURE 5-9 The factors F_V, F_L, and F_R as functions of the ratio ℓ_c/ℓ_r (length of the coil to length of the rod). These factors were determined from averages of experimental data.

The internal impedance of the conductor Z^i is assumed to be the same as that for the unloaded loop. The empirical factors F_R and F_L in Eqs. 5-18 and 5-19, like F_V, were determined from an average of experimental results and are also shown as a function of the ratio ℓ_c/ℓ_r in Figure 5-9.[10,11] It should be emphasized that the graphs for the three factors F_V, F_R, and F_L represent typical measured values and show only the dependence on the ratio ℓ_c/ℓ_r; some dependence on the other parameters describing the coil and the rod is to be expected.

Equations 5-16 through 5-19 provide a complete description of the electrically small ferrite-loaded receiving loop (single-layer solenoidal coil with a cylindrical core). Other parameters of interest, such as the Q of the antenna, can be determined from these results. The permeability of a specific ferrite can be obtained from the manufacturer or from the extensive tables and charts in *Soft Ferrites: Properties and Applications* by E. C. Snelling.[11] The many parameters that are to be chosen for the ferrite-loaded loop, such as μ_r', ℓ_r, ℓ_c, N, etc., offer a great deal of flexibility in its design. Several discussions in the literature determine these parameters to optimize the performance for a particular application.[12]

The electromagnetic field of the ferrite-loaded transmitting loop is given by Eqs. 5-1 to 5-3 with the moment $m = \mu_{\text{rod}} F_V I_0 NA$. The ferrite-loaded loop, however, is seldom used as a transmitting antenna because of the problems associated with the nonlinearity and the dissipation in the ferrite at high magnetic field strengths.[13]

Matching Networks

A matching network is generally used to improve the power transfer to and from the electrically small loop antenna. At the frequency ω_0, the impedance of the loop can be transformed to the resistance R_0 by using various networks, two of which are shown in Figure 5-10.[14] In both arrangements, the capacitor C_1 is used to bring the loop close to resonance at ω_0. Then the additional elements (the capacitor C_2 in Figure 5-10*a*, or the spacing s_2 and length of the lines l_2 in Figure 5-10*b*) are adjusted to make the impedance R_0. The matches obtained with these simple networks generally have very narrow bandwidth.

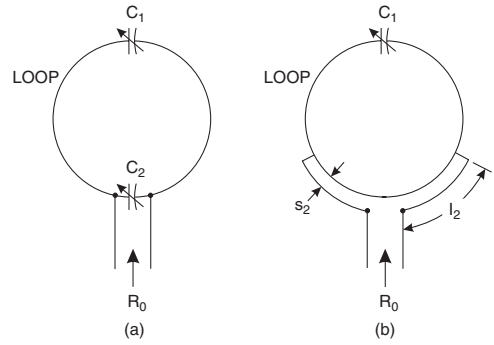

FIGURE 5-10 Examples of matching networks used with electrically small loop antennas. Matching to the resistance R_0 with (*a*) two capacitors and with (*b*) shunt feed and one capacitor.

The capacitors for the circuit in Figure 5-10*a* are

$$C_1 = \frac{1}{\omega_0\left(\omega_0 L - R\sqrt{R_0/R - 1}\right)} \approx \frac{1}{\omega_0\left(\omega_0 L - \sqrt{RR_0}\right)} \tag{5-20}$$

$$C_2 = \frac{1}{\omega_0 R_0}\sqrt{R_0/R - 1} \approx \frac{1}{\omega_0\sqrt{RR_0}} \tag{5-21}$$

in which the approximations on the right apply for the practical case $R_0/R \gg 1$. Figure 5-10*b* is for a symmetrical shunt-driven loop. Sometimes an asymmetrical configuration is used, in which the length of one of the two lines is set to zero.

5.3 ELECTRICALLY LARGE LOOPS

As the electrical size of the loop antenna is increased, the current distribution in the loop departs from the simple uniform distribution of the electrically small loop. For single-turn loops, this departure has a significant effect on performance when the circumference is greater than about 0.1λ. For example, the radiation resistance of an electrically small circular loop with a uniform current, as predicted by Eq. 5-5, is about 86 percent of the actual resistance when $\beta b = 2\pi b/\lambda = 0.1$ and only about 26 percent of the actual resistance when $\beta b = 0.3$.

Of the possible shapes for an electrically large loop antenna, the single-turn thin-wire circular loop has received the most attention, both theoretical and experimental. The popularity of the circular loop is due in part to its straightforward analysis by expansion of the current in the loop as a Fourier series:

$$I(\phi) = I_0 + 2\sum_{n=1}^{m} I_n \cos n\phi \tag{5-22}$$

in which the angle ϕ is defined in Figure 5-1.[15] Measurements on electrically large loops with other shapes, such as the square loop, show that their electrical performance is qualitatively similar to that of the circular loop; therefore, only the circular loop will be discussed here.[16]

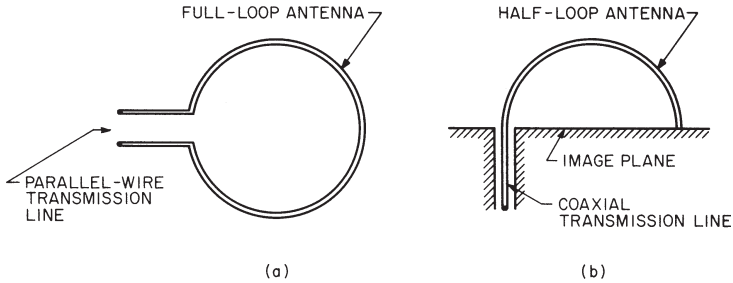

FIGURE 5-11 Methods of driving the circular-loop antenna: (*a*) Full-loop antenna driven from parallel-wire transmission line; (*b*) Half-loop antenna driven from coaxial transmission line

Circular-Loop Antenna

The theoretical model for the circular-loop antenna generally assumes a point-source generator of voltage V at the position $\phi = 0$, making the input impedance of the loop $Z = R + jX = V/I(\phi = 0)$. In practical applications, the full-loop antenna is usually driven from a balanced source, such as a parallel-wire transmission line, and the half-loop antenna, the analog of the electric monopole, is driven from a coaxial line, as in Figure 5-11. The point-source generator of the theoretical model contains no details of the geometry of the feed point, and it is not strictly equivalent to either of these methods of excitation. However, theoretical current distributions, input impedances, and field patterns computed with the point-source generator and 20 terms in the Fourier series (Eq. 5-22) are generally in good agreement with measured values.* Thus, the theory serves as a useful design tool.

For the half-loop antenna (Figure 5-11*b*), an accurate analysis, based on the Fourier series, is available that includes the details of the feeding coaxial line.[17] Results from this analysis are in excellent agreement with measurements and show such things as the change in the input impedance of the half-loop antenna with a change in the characteristic impedance of the feeding coaxial line.

In Figures 5-12 and 5-13, the input impedance of a loop constructed from a perfect conductor is shown as a function of the electrical size of the loop $\beta b = 2\pi b/\lambda$ (circumference/wavelength) for various values of the radius of the conductor, indicated by the *thickness parameter* $\Omega = 2\ln(2\pi b/a)$. These impedances are for full-loop antennas; for half-loop antennas with the same radius and conductor size, impedances are approximately one-half of these values. The reactance X is seen to be zero at points near $\beta b = \frac{1}{2}, \frac{3}{2}, \frac{5}{2}, \ldots$ (antiresonant points) and $\beta b = 1, 2, 3, \ldots$ (resonant points). The resistance obtains relative maxima near the points of antiresonance and relative minima near the points of resonance. Impedances computed from Eqs. 5-5 and 5-7, which apply to electrically small loops, are also shown in Figures 5-12 and 5-13; the inaccuracy of these formulas with increasing βb is evident.

When the electrical size of the loop is near that for resonance ($\beta b = 1, 2, 3, \ldots$), the dominant term in the Fourier series for the current (Eq. 5-22) is the one with n = integer (βb). For example, near the first resonance $\beta b \approx 1$, the current in the loop is approximately $I(\phi) = 2I_1 \cos\phi$, and the loop is commonly referred to as a resonant loop. The resonant loop ($\beta b \approx 1$) is the most frequently used electrically large loop. It has a reasonable input resistance, $R \approx 100\ \Omega$, for matching to a transmission line, particularly when compared with the resistance of the antiresonant loop ($\beta b \approx 0.5$), which may be larger than 10 kΩ.

*The theoretical results in Figures 5-12, 5-13, 5-15 to 5-19, and 5-21 were computed by the author by using 20 terms in this series.

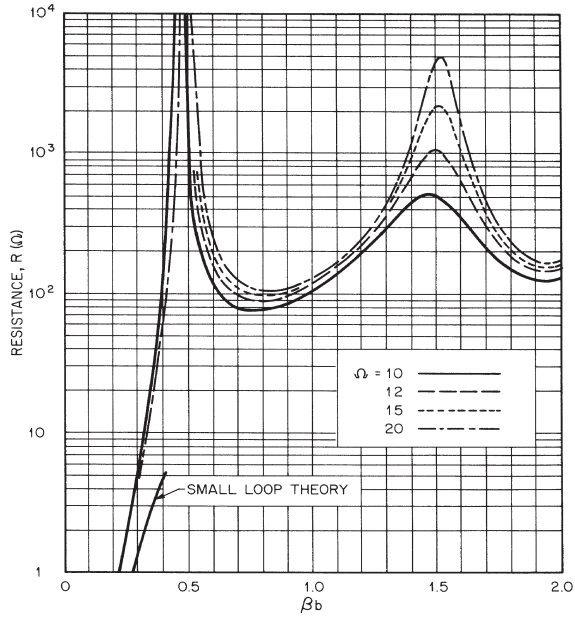

FIGURE 5-12 Input resistance of circular-loop antenna versus electrical size (circumference/wavelength)

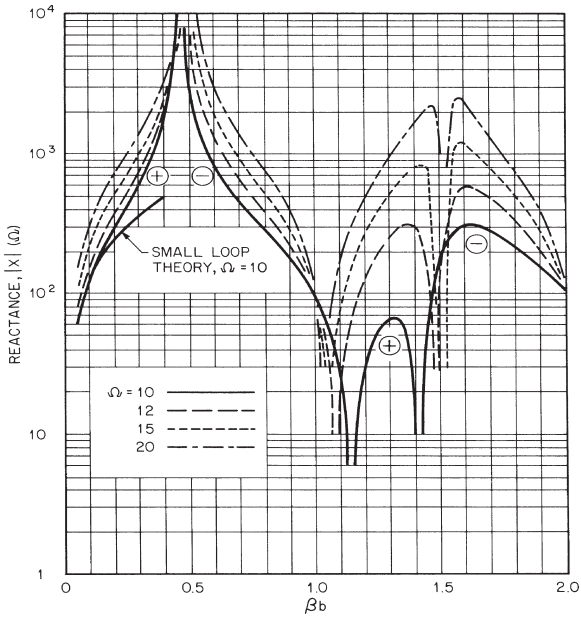

FIGURE 5-13 Input reactance of circular-loop antenna versus electrical size (circumference/wavelength)

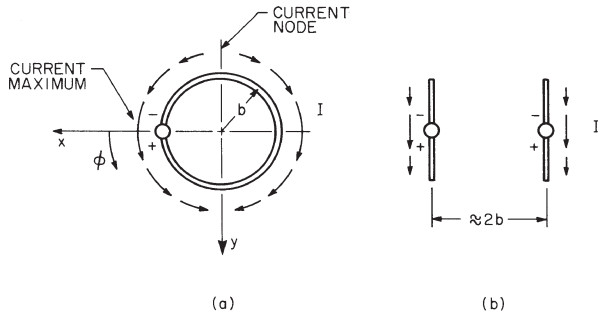

FIGURE 5-14 Schematic of current distribution in (*a*) resonant loop and in (*b*) the approximately equivalent pair of dipoles

Resonant Circular Loop

The current in the resonant loop has maxima at the generator, $\phi = 0$, and at the diametrically opposite point, $\phi = \pi$, with nodes at $\phi = \pi/2$ and $3\pi/2$. On examination of Figure 5-14, the current is seen to be roughly equivalent to that in a pair of parallel dipole antennas driven in phase and with a spacing approximately equal to the diameter of the loop.

The far-zone field patterns for the resonant loop shown in Figure 5-15*a–c* are also similar to those for the pair of dipoles; they have little resemblance to the figure-eight pattern of the electrically small loop, Figure 5-2. There are two components to the electric field, E_θ and E_ϕ. E_θ is zero in the horizontal plane $\theta = \pi/2$ and in the vertical plane $\phi = 0$, π, while E_ϕ is small in the vertical plane $\phi = \pi/2$, $3\pi/2$. The amplitude patterns are symmetrical about

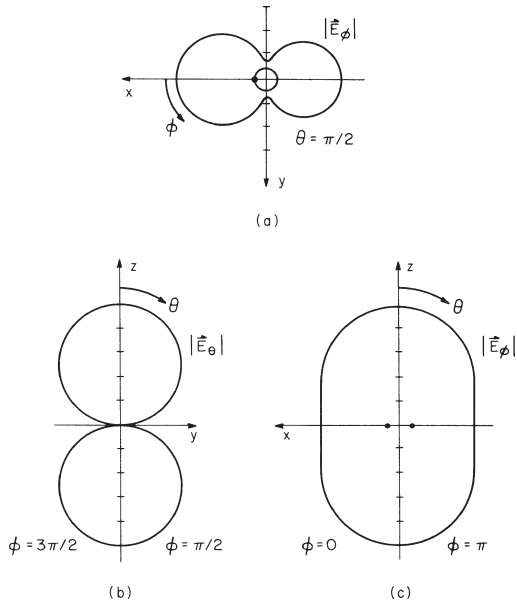

FIGURE 5-15 Far-zone electric field for loop with βb = 1.0, Ω = 10: (*a*) Horizontal-plane field pattern $|\mathbf{E}_\phi|$, $\theta = \pi/2$; (*b*) Vertical-plane field pattern $|\mathbf{E}_\theta|$, $\phi = \pi/2$, $3\pi/2$; (*c*) Vertical-plane field pattern $|\mathbf{E}_\phi|$, $\phi = 0$, π

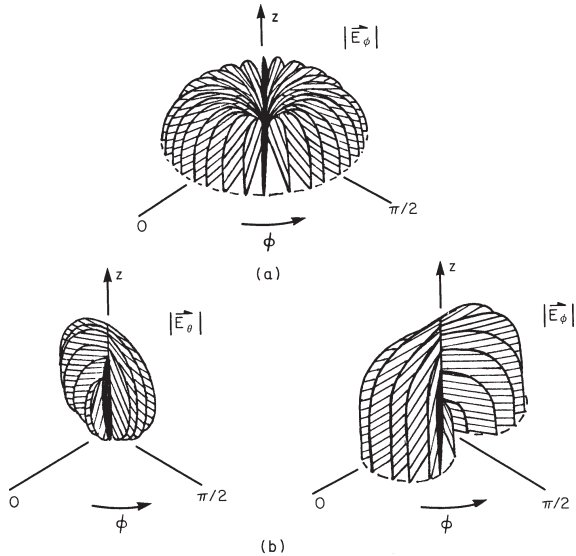

FIGURE 5-16 Far-zone electric field patterns in upper hemisphere: (*a*) Electrically small loop, $\beta b = 1$; (*b*) Resonant loop, $\beta b = 1.0$

the plane $\theta = \pi/2$ and $\phi = 0, \pi$ owing to the geometrical symmetry of the loop, and they are nearly symmetrical about the plane $\phi = \pi/2, 3\pi/2$, because of the dominance of the term $2I_1 \cos \phi$ in the current distribution. At the maxima ($\theta = 0, \pi$) of the bidirectional pattern, the electric field is linearly polarized in the direction $\hat{\mathbf{y}}$.

To help with the visualization of the electric field, three-dimensional amplitude patterns for the electrically small loop and the resonant loop are presented in Figure 5-16. Each drawing is a series of patterns on planes of constant angle ϕ; only the patterns in the upper hemisphere ($0 \le \theta \le \pi/2$) are shown, since those in the lower hemisphere are identical.

The directivity of the circular loop in the direction $\theta = 0$ or π is shown as a function of the electrical size βb in Figure 5-17; it is about 3.4 dB for $\beta b = 1.0$ and has a maximum of about 4.5 dB for $\beta b = 1.4$. The directivity is fairly independent of the parameter Ω for $\beta b \le 1.4$.

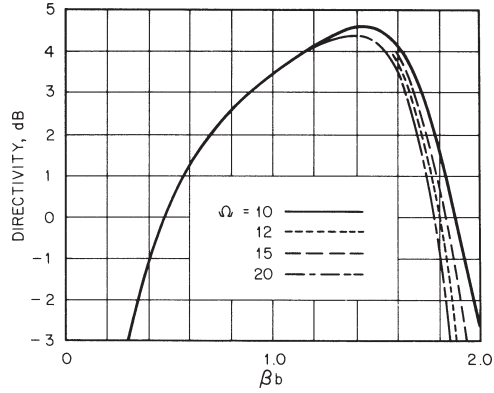

FIGURE 5-17 Directivity of circular-loop antenna for $\theta = 0$, π versus electrical size (circumference/wavelength)

The resonant loop antenna is attractive for practical applications because of its moderate input resistance and symmetrical field pattern with reasonable directivity. The bidirectional nature of its pattern, however, is usually not desired, and a reflector or an array of loops is used to make the pattern unidirectional.

For most antenna problems, the far-zone field described previously is of interest; however, for some applications the field close to the loop may be required. Expressions for the near field of the circular-loop antenna with uniform current or the Fourier series representation in Eq. 5-22 have been obtained using various methods.[18]

Circular Loop with Planar Reflector

The pattern of the resonant loop is made unidirectional and the directivity in the direction $\theta = 0$ is increased by placing the loop over a planar reflector. The theoretical results for an infinite perfectly conducting reflector (Figure 5-18) show that the directivity is greater than 9 dB for spacings between the loop and the reflector in the range $0.05 \le d/\lambda \le 0.2$.[19] Over this same range of spacings, the input impedance $Z = R + jX$ (Figure 5-19) has values that are easily matched: the resistance is reasonable ($R \le 135\ \Omega$), and the reactance is small ($|X| \le 20\ \Omega$).

The theoretical results for an infinite reflector are in good agreement with measured data for finite square reflectors of side length s. The directivities measured by Adachi and Mushiake[20] (Figure 5-18) for a reflector with $s/\lambda = 1.2$ and $d/\lambda \le 0.26$ are slightly higher than those for an infinite plane, while the input impedances measured by Rojarayanont and Sekiguchi[21] (Figure 5-19) show variations with reflector size, $0.48 \le s/\lambda \le 0.95$, but general agreement with the results for an infinite plane.

Electric field patterns measured by Rojarayanont and Sekiguchi[21] for resonant loops one-quarter wavelength, $d/\lambda = 0.25$, in front of square reflectors are shown in Figure 5-20. The shaded area in each figure shows the variation in the pattern that is a result of changing the size of the square reflector from $s/\lambda = 0.64$ to $s/\lambda = 0.95$.

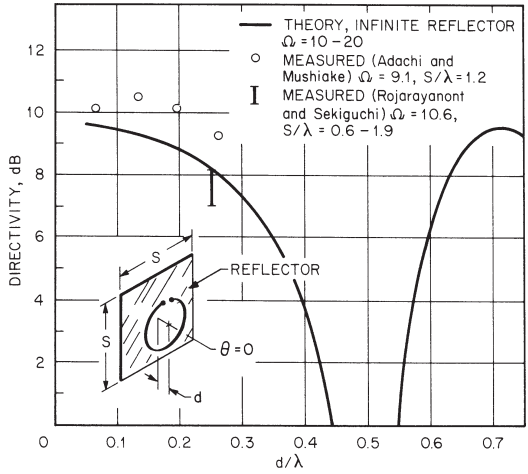

FIGURE 5-18 Directivity of circular-loop antenna, $\beta b = 1.0$, for $\theta = 0$ versus distance from reflector d/λ. Theoretical curve is for infinite planar reflector; measured points are for square reflector.

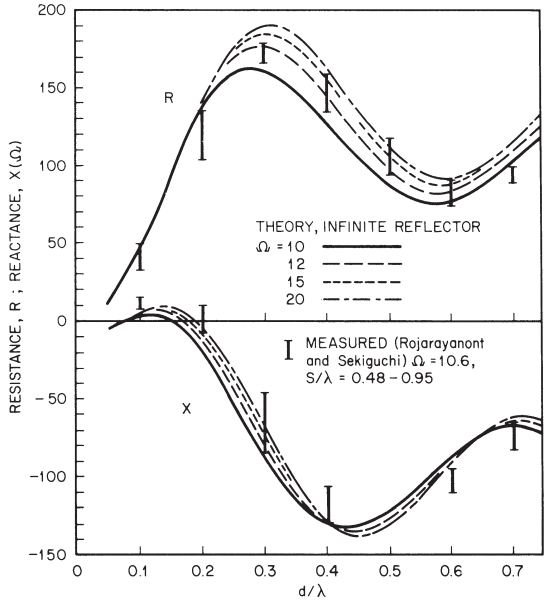

FIGURE 5-19 Input impedance of circular-loop antenna, $\beta b = 1.0$, versus distance from reflector d/λ. Theoretical curves are for infinite planar reflector; measured points are for square reflector.

Coaxial Arrays of Circular Loops

Loop antennas, like linear antennas, can be combined in an array to improve performance. The most common array of circular loops is the coaxial array in which all the loops are parallel and have their centers on a common axis; an example of a coaxial array

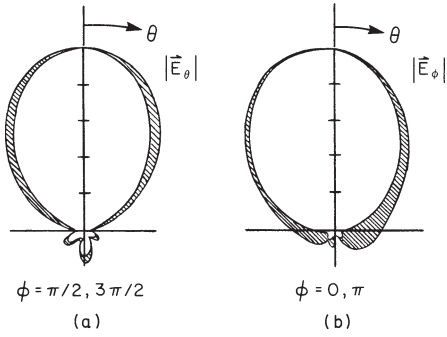

FIGURE 5-20 Measured far-zone electric field patterns for loop with $\beta b = 1.0$ over square reflector, $d/\lambda = 0.25$. Inner curve $s/\lambda = 0.95$; outer curve $s/\lambda = 0.64$. (*a*) Vertical-plane field pattern $|\mathbf{E}_\theta|$, $\phi = \pi/2, 3\pi/2$. (*b*) Vertical-plane field pattern $|\mathbf{E}_\phi|$, $\phi = 0, \pi$. (*Measured data from Rojarayanont and Sekiguchi*)

is shown later in the inset of Figure 5-22. The Fourier-series analysis for the single loop is easily extended to the coaxial array when all the driven loops are fed at a common angle, e.g., $\phi = 0$ in Figure 5-1. The current distribution in each loop is expressed as a series of trigonometric terms like that in Eq. 5-22. The simplicity of the analysis results from the orthogonality of the trigonometric terms, which makes the coupling between loops occur only for terms of the same order n. Thus, if all the driven loops in the array are near resonant size, $\beta b \approx 1$, the term $n = 1$ is the dominant one in the current distributions for all loops; i.e., the current is approximately proportional to cos ϕ in all loops.

When all the elements in the loop array are driven, the same procedures that are used with arrays of linear elements can be applied to select the driving-point voltages to optimize certain parameters, such as directivity.[22] The feed arrangement needed to obtain the prescribed driving-point voltages, however, is very complex for more than a few elements in the array. As a result, a simpler and more economical arrangement, an array containing only one driven element and several parasitic loops, is often used (a *parasitic loop* is a continuous wire with no terminals).

When a single, closely spaced parasite is used with a driven loop, the parasite may act as a director or as a reflector. This is illustrated in Figure 5-21, in which electric field patterns are shown for a driven loop ($\beta b_2 = 1.0$) and a parasitic loop with the spacing $d/\lambda = 0.1$. For loops of the same electrical size ($\beta b_1 = \beta b_2 = 1.0$), the maxima in the pattern at $\theta = 0, \pi$ are nearly equal. The parasitic loop that is slightly smaller than the driven loop ($\beta b_1 = 0.95$) acts as a director, producing a maximum in the pattern at $\theta = \pi$, while the parasitic loop that is slightly larger than the driven loop ($\beta b_1 = 1.05$) acts as a reflector, producing a maximum in the pattern at $\theta = 0$. This behavior is very similar to that observed for a resonant linear antenna with a closely spaced parasite.

The driven loop of electrical size $\beta b_2 = 1.2$ ($\Omega_2 = 11$, $a_1 = a_2$) with a single parasite was studied in detail by Ito et al.[23] In that study, the optimum director was determined to be a loop with $\beta b_1 \approx 0.95$ and spacing $d/\lambda \approx 0.10$. This produced a directivity of about 7 dB at $\theta = \pi$. The optimum reflector was a loop with $\beta b_1 \approx 1.08$ and a spacing $d/\lambda \approx 0.15$. This produced a directivity of about 8 dB at $\theta = 0$. Note that, for this case, the optimum director and the optimum reflector are both smaller than the driven loop.

A Yagi-Uda array of loops with a single reflector (element 1), an exciter (the driven element 2), and several directors of equal size βb and equal spacing d/λ is shown in the

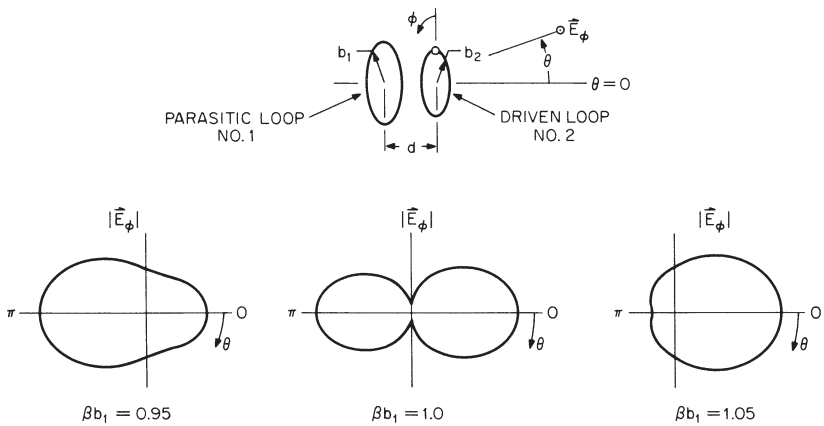

FIGURE 5-21 Far-zone electric field patterns $|\mathbf{E}_\phi|$ in plane $\phi = 0, \pi$ for driven loop with single parasite, $\beta b_2 = 1.0$, $d/\lambda = 0.1$, $\Omega_1 = \Omega_2 = 20$

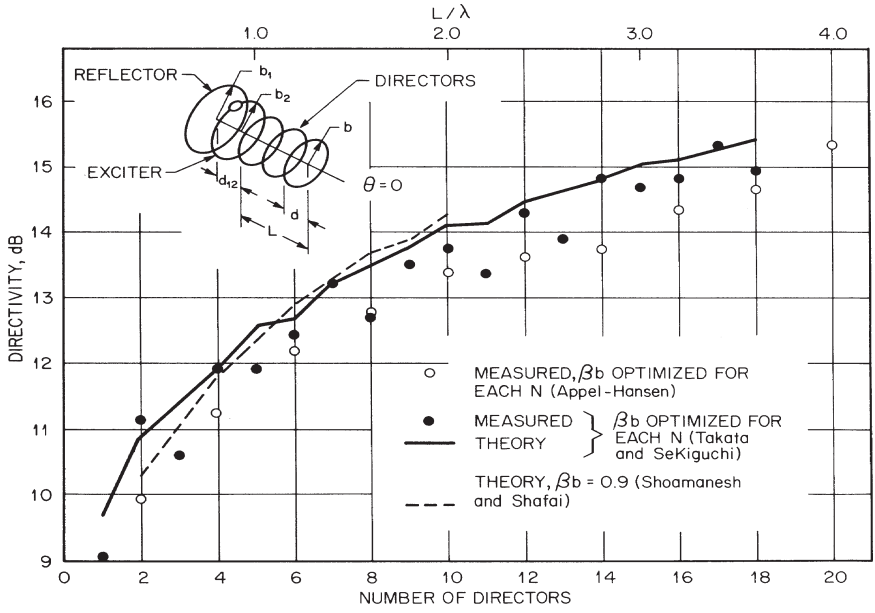

FIGURE 5-22 Directivity of Yagi-Uda array of circular-loop antennas for $\theta = 0$ versus number of directors, director spacing $d/\lambda = 0.2$

inset of Figure 5-22.* As in its counterpart with linear elements, in the Yagi-Uda array of loops the reflector-exciter combination acts as a feed for a slow wave that propagates along the array of directors.[24] The lowest-order propagating wave (mode) exists for directors less than about resonant size ($\beta b \leq 1.0$) with spacings less than about a half wavelength ($d/\lambda \leq 0.5$).[25] An array supporting this mode has an end-fire pattern with a linearly polarized electric field at the maximum, $\theta = 0$.

The procedure for designing a Yagi-Uda array of loops is the same as for an array with linear elements.[26] The isolated reflector-exciter combination is usually chosen to have maximum directivity in the direction $\theta = 0$. For example, the optimized two-element array described previously might be used. The number, size, and spacing of the directors are then adjusted to obtain the desired performance, such as specified end-fire directivity. The maximum end-fire directivity is determined by the electrical length of the array L/λ (L is the distance from the exciter to the last director). The larger the number of directors within the length L, the smaller the electrical size of the directors will be for maximum directivity, typically $0.8 \leq \beta b \leq 1.0$.

As an example, the directivity of a Yagi-Uda array of loops with the director spacing $d/\lambda = 0.2$ is shown as a function of the number of directors or the length of the array L/λ in Figure 5-22. Two theoretical curves and two sets of measured data are shown. All the results agree to within about 1 dB, even though they are for different reflector-exciter combinations and slightly different director sizes.†

*In the literature of amateur radio the Yagi-Uda array of loops, usually square loops, is referred to as a *quad antenna*.

†The parameters used by the different investigators are Appel-Hansen, $\beta b_1 = \beta b_2 = 1.10$, d_{12}/λ optimized for the isolated reflector-exciter, and βb optimized for each length L/λ; Takata and Sekiguchi, $\beta b_1 = 1.05$, $\beta b_2 = 1.20$, $d_{12}/\lambda = 0.15$, and βb optimized for each length L/λ; Shoamanesh and Shafai (1979), $\beta_1 b = 1.05$, $\beta b_2 = 1.10$, $d_{12}/\lambda = 0.1$, and $\beta b = 0.9$ for all lengths L/λ.

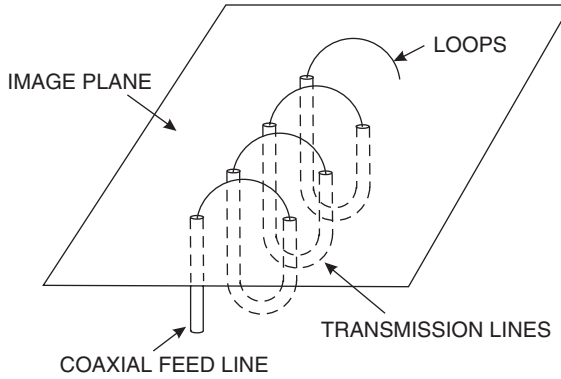

FIGURE 5-23 Coaxial array of half-loop antennas. Spacing between loops and lengths of interconnecting transmission lines can be adjusted to change field pattern of the array.

Arrays can also be formed using the half-loop antenna shown in Figure 5-11*b* as the element.[27] The coaxial loops can be fed individually, used as parasites, or they can be connected in series by transmission lines below the image plane and fed at a single point, as in Figure 5-23. In this arrangement, the spacing between the loops and the lengths of the transmission lines can be adjusted to change the field pattern of the array.

5.4 SHIELDED-LOOP ANTENNA

For certain applications it is desirable to position the terminals of the loop antenna precisely so as to produce geometrical symmetry for the loop and its connections about a plane perpendicular to the loop. This can often be accomplished by using the so-called shielded loop. Figure 5-24*a* is an example of a shielded receiving loop whose external surface is symmetrical about the *yz* plane.[28]

With reference to Figure 5-24*a*, the thickness of the metal forming the shield is chosen to be several skin depths; this prevents any direct interaction between the currents on the internal and the external surfaces of the shield. The effective terminals of the loop antenna are at the ends of the small gap *AB*. The inner conductor and the shield form a coaxial transmission line of length $h + \pi b$ connecting the gap with the load impedance Z_S. Thus, the effective load impedance Z_L at the gap is Z_S transformed by the length of transmission line $h + \pi b$.

The receiving antenna in Figure 5-24*a* is easily analyzed by considering the loop, Figure 5-24*b*, and the transmission line, Figure 5-24*c*, separately. The incident field produces a current on the external surface of the shield; the current passes through the effective impedance Z_L, producing the voltage V_L, which for an electrically small loop can be determined from Eqs. 5-12 and 5-14. This voltage is transmitted over the coaxial line to become V_S at the load impedance Z_S.

Other examples of the shielded loop are shown in Figure 5-25. A balanced version of the loop in Figure 5-24*a* is in Figure 5-25*a*, and a method for feeding a loop in front of a planar reflector is in Figure 5-25*b*.

To illustrate a typical use of the shielded loop, consider the electrically small receiving loop placed in an incident linearly polarized electromagnetic plane wave with the wave

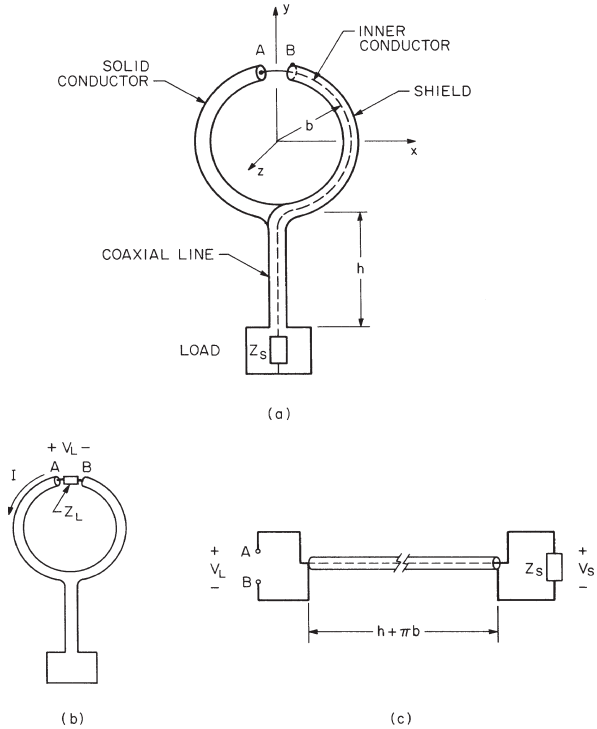

FIGURE 5-24 (*a*) Shielded-loop antenna (*b*) with equivalent antenna and (*c*) equivalent transmission line

vector $\mathbf{k}_i$, as in Figure 5-26. This is the same geometry as in Figure 5-5, except that the terminals of the loop are at the angle $\phi = \phi_L$ instead of $\phi = 0$, and $\phi_i = \pi$, $\psi_i = 0$. The loop in this example might be an antenna in a direction finder with the direction of the incident wave to be determined by placing a null of the field pattern in the direction of $\mathbf{k}_i$.

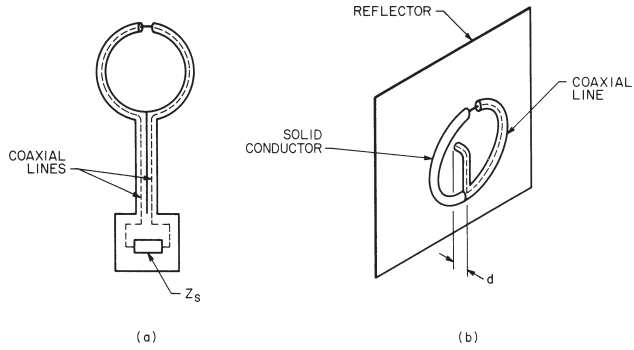

FIGURE 5-25 (*a*) Balanced shielded-loop antenna and (*b*) method of feeding loop antenna in front of planar reflector

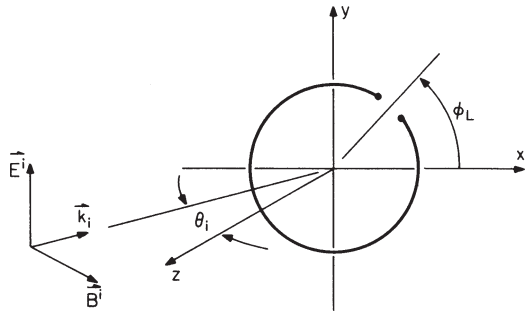

FIGURE 5-26 Receiving loop in plane-wave incident field

The voltage at the open-circuited terminals of the electrically small loop, determined from the Fourier-series analysis, is approximately*

$$V_{OC} = j\omega AB^i(\sin\theta_i - 2j\beta b\cos\phi_L) \tag{5-23}$$

For many applications, the second term in Eq. 5-23 is negligible, since $\beta b \ll 1$ for an electrically small loop. In other applications, however, this term may represent a significant contribution to the response. For example, the sensitivity of the antenna in the direction finder is decreased by this term because it fills in the nulls of the sin θ_i field pattern (for $\beta b = 0.1$, $\phi_L = 0$, the minima in the pattern are only 14 dB below the maxima).

The second term in Eq. 5-23 can be made insignificant by reducing the electrical size of the loop βb; however, this will also decrease the sensitivity, because the area of the loop is decreased. An alternative is to make this term zero by placing the terminals of the loop precisely at $\phi_L = \pm \pi/2$ (cos $\phi_L = 0$). This can be accomplished by using a shielded loop as in Figure 5-24*a* or Figure 5-25*a*.

5.5 PULSE-EXCITED CIRCULAR-LOOP ANTENNA

In the treatment presented so far, the performance of the loop antenna has been described for harmonic time dependence, which is the case for most practical applications. However, there are instances when the loop antenna is used with pulse excitation, such as in some proposed ultra-wideband communications systems. With pulse excitation, the time delay between pulses can be used to identify the radiation from different points on the loop, and this provides some physical insight into how the loop radiates energy. The details for the calculations are in the literature,[29] and only a qualitative description for the radiation will be given here.[30]

When the circular loop is excited by a voltage pulse, such as a Gaussian, pulses of charge travel around the loop at roughly the speed of light, c: a positive pulse travels in the clockwise direction, and a negative pulse travels in the counterclockwise direction, as shown in Figure 5-27*a*. When these pulses have traveled once around the loop, they return to the source, where they are partially absorbed and partially transmitted, as shown in Figure 5-27*b*. This process is repeated until there is no more charge left on the loop.

*Eq. 5-23 is a more accurate formula than Eq. 5-12, which is also for the open-circuited voltage of the electrically small loop. It contains an additional term not in Eq. 5-12, the second term in the parentheses, which is proportional to βb. When $\beta b \ll 1$, Eq. 5-23 reduces to Eq. 5-12 with $N = 1$, and $\psi_i = 0$.

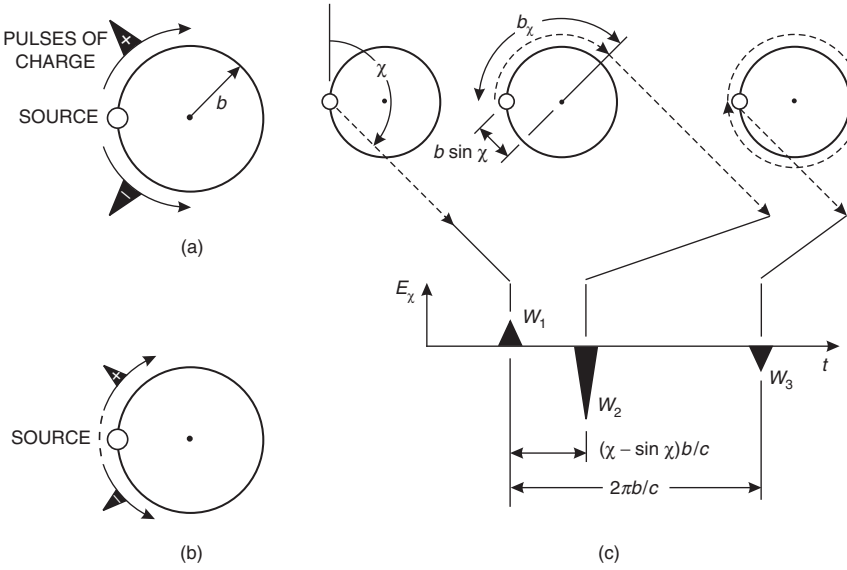

FIGURE 5-27 Schematic drawings for pulse-excited circular-loop antenna. (*a*) Pulses of charge leaving source and traveling around loop. (*b*) Pulses of charge after completing one trip around loop and passing through source. (*c*) Time history of far-zone electric field radiated by loop. Results are shown in the plane of the loop for the radiation due to the positive pulse of charge making one trip around the loop.

The far-zone electric field produced by one of these pulses of charge, the positive one traveling in the clockwise direction once around the loop, is described schematically in Figure 5-27*c*. For this example, the width of the pulse is small compared with the time for light to travel around the perimeter of the loop ($2\pi b/c$), and the time history of the field is shown for one angle of observation in the plane of the loop, $\chi = 3\pi/4 = 135°$.

Three wavefronts can be distinguished in Figure 5-27*c*.[30] The wavefronts W_1 and W_3 are produced when the pulse of charge leaves the source and when it is absorbed/transmitted at the source, respectively. The wavefront W_2 is continuously produced as the pulse propagates around the loop. Wavefront W_2 appears to originate at a point on the loop where the tangent line to the loop points in the direction of the observer. As indicated in the figure, this can be ascertained from the time of arrival of W_2 relative to W_1. The radiation from the negative pulse of charge in Figure 5-27*a* and from all of the subsequent pulses, Figure 5-27*b*, can be obtained in a similar manner.

A simple analogy can be constructed between the radiation from this loop and the radiation from a moving point charge.[30] The radiation arising at the source, wavefronts W_1 and W_3, is analogous to the radiation that occurs when a point charge is accelerated in a direction parallel to its velocity (*bremsstrahlung*), and the radiation that occurs along the loop, wavefront W_2, is analogous to the radiation that occurs when a point charge is accelerated in a direction normal to its velocity (*synchrotron radiation*).

When the loop is excited with a time–harmonic signal, a cosinusoid, each half of the cosinusoid can be considered to be a pulse. The radiation is then that due to a train of positive and negative pulses of charge—the positive pulses being separated in time by the period of the cosinusoid, $T = 2\pi/\omega = \lambda/c$. Notice that the charge on the loop from consecutive positive pulses will add when the travel time around the loop is T. This occurs for $\beta b = 2\pi b/\lambda = 1$, which is the condition for resonance stated earlier in connection with the input impedance of the loop.

In practical applications, it may be desirable to eliminate or reduce the amplitude of some of the pulses radiated by the loop. This can be accomplished by incorporating discrete or continuous resistive loading along the wire of the loop.[30,31]

5.6 ADDITIONAL TOPICS

The brevity of this review requires omission of many interesting topics concerning loop antennas. In recent years there has been considerable study of loop antennas in close proximity to or embedded in material media such as the ocean, the earth, and biological tissue. The electrical characteristics of loops in these instances can be quite different from those of loops in unbounded free space, as described in this review. The major applications of this work are in the areas of subsurface communication and detection (geophysical prospecting) and the study of the interaction of electromagnetic radiation with biological systems.

The loop antenna near a planar interface separating two semi-infinite material regions, such as the air and the earth, has been investigated extensively. When the loop is electrically small, it can be approximated by an elementary magnetic dipole, and the electromagnetic field away from the loop can be determined from the classical analysis of Sommerfeld.[32] If the field near the electrically small loop is required, the approximation by a magnetic dipole may no longer be adequate, and a loop with a finite radius and a uniform current must be considered.[33] For the electrically large loop near a planar interface, an analysis that allows a nonuniform current in the loop, such as the Fourier-series analysis for the circular loop,[34] must be used.

The performance of a loop embedded in a material can be altered significantly by placing the loop in a dielectric cavity, such as a sphere, to form an insulated loop. The electrical size and shape of the insulating cavity and the location of the loop in the cavity can be used to control the electromagnetic field and input impedance of the antenna.[35]

Models have been developed to analyze a loop antenna placed near the human body, and the results have been used for two different purposes.[36] In one case the concern is the possible hazard due to the electromagnetic energy deposited in the body. In the other case the concern is the effect the body has on the performance (impedance and pattern) of a loop antenna contained in a personal communications device, such as a pager.

REFERENCES

1. H. Hertz, *Electric Waves* (London: Macmillan and Co., Ltd., 1893).
2. R. G. Medhurst, "H.F. Resistance and Self-Capacitance of Single-Layer Solenoids," *Wireless Eng*., vol. 24 (March 1947): 80. The measurements of Medhurst show that the self-resonance of a solenoid with $\ell_c/2b \geq 3$ occurs at a wavelength at which $N\beta b \geq 0.4$. The current distribution in the solenoid is assumed to be uniform well below self-resonance, i.e., $N\beta b \leq 0.1$.
3. The electrically small loop antenna in free space is discussed in many textbooks; see, for example, G. S. Smith, *An Introduction to Classical Electromagnetic Radiation* (Cambridge, UK: Cambridge University Press, 1997): 477–485; R. W. P. King, *Fundamental Electromagnetic Theory* (New York: Dover Publications, Inc., 1963): 441–457; and S. A. Schelkunoff and H. T. Friis, *Antennas: Theory and Practice* (New York: John Wiley & Sons, Inc., 1952): 319–324.
4. Formulas and graphs for the internal impedance per unit length of round conductors are in S. Ramo, J. R. Whinnery, and T. Van Duzer, *Fields and Waves in Communication Electronics* (New York: John Wiley & Sons, Inc., 1965): 286–297.
5. G. S. Smith, "Radiation Efficiency of Electrically Small Multiturn Loop Antennas," *IEEE Trans. Antennas Propagat*., vol. AP-20 (September 1972): 656.

6. F. W. Grover, *Inductance Calculations: Working Formulas and Tables* (New York: D. Van Nostrand Company, Inc., 1946).
7. Internal resonance transverse to the axis of an infinitely long magnetic rod is discussed in L. Page, "The Magnetic Antenna," *Phys. Rev*., vol. 69 (June 1946): 645.
8. The graph in Figure 5-8 was constructed by using the static demagnetizing factor for a cylindrical rod as presented in R. M. Bozorth and D. M. Chapin, "Demagnetizing Factors of Rods," *J. App. Phys*., vol. 13 (May 1942): 320; also R. M. Bozorth, *Ferromagnetism* (New York: D. Van Nostrand Company, Inc., 1951): 845–849; and G. A. Burtsev, "Computing the Demagnetizion Coefficient of Cylindrical Rods," *Soviet J. Nondestructive Test. (Defektoskopiya)*, vol. 5 (September–October 1971): 499.
9. The receiving loop with a spheroidal core is discussed in R. E. Burgess, "Iron-Cored Loop Receiving Aerial," *Wireless Eng.*, vol. 23 (June 1946): 172; J. R. Wait, "Receiving Properties of Wire Loop with a Spheroidal Core," *Can. J. Tech.*, vol. 31 (January 1953): 9, and "The Receiving Loop with a Hollow Prolate Spheroidal Core," *Can. J. Tech.*, vol. 31 (June 1953): 132; V. H. Rumsey and W. L. Weeks, "Electrically Small, Ferrite-Loaded Loop Antennas," *IRE Conv. Rec*., Part 1 (1956): 165; and E. J. Scott and R. H. DuHamel, "Effective Permeability of Spheroidal Shells," Tech. Rep. 9, Antenna Lab., University of Illinois, Urbana (1956).
10. The customary procedure for analyzing the solenoidal coil with a cylindrical ferrite core is in H. van Suchtelen, "Ferroxcube Aerial Rods," *Electron. Appl. Bull*., vol. 13 (June 1952): 88. Extensions of this procedure and additional measured data are in J. S. Belrose, "Ferromagnetic Loop Aerials," *Wireless Eng*., vol. 32 (February 1955): 41; and J. Dupuis, "Cadres utilisant des ferrites," *L'onde électrique*, vol. 35 (March–April 1955): 379.
11. E. C. Snelling, *Soft Ferrites: Properties and Applications* (Cleveland: CRC Press, 1969): 182–192, 327–336.
12. There are many journal articles in addition to those in Refs. 9 through 11 that discuss the design and optimization of ferrite-loaded loop antennas for broadcast receivers; an incomplete list follows: H. Blok and J. J. Rietveld, "Inductive Aerials for Modern Broadcast Receivers," *Philips Tech. Rev*., vol. 16 (January 1955): 181; W. J. Polydoroff, *High-Frequency Magnetic Materials, Their Characteristics and Principal Applications* (New York: John Wiley & Sons, Inc., 1960): 163–179; E. J. Maanders and H. van der Vleuten, "Ferrite Aerials for Transistor Receivers," *Philips Matronics Tech. Info. Bull*. (February 1961): 354; H. J. Laurent and C. A. B. Carvalho, "Ferrite Antennas for A.M. Broadcast Receivers," *IRE Trans. Broadcast Telev. Receivers*, vol. BTR-8 (July 1962): 50; G. Schiefer, "A Small Ferroxcube Aerial for VHF Reception," Philips Tech. Rev., vol. 24 (1962–1963): 332; I. D. Stuart, "Practical Considerations in the Design of Ferrite Cored Aerials for Broadcast Receivers," *IREE Proc. (Australia)*, vol. 27 (December 1966): 329; R. C. Pettengill, H. T. Garland, and J. P. Meindl, "Receiving Antenna Design for Miniature Receivers," *IEEE Trans. Antennas Propagat*., vol. AP-25 (July 1977): 528.
13. The ferrite-loaded transmitting loop is discussed in R. DeVore and P. Bohley, "The Electrically Small Magnetically Loaded Multiturn Loop Antenna," *IEEE Trans. Antennas Propagat*., vol. AP-25 (July 1977): 496.
14. K. H. Patterson, "Down-to-Earth Army Antenna," *Electronics* (August 1967): 111; and R. W. P. King, "The Shunt-Driven Circular Loop Antenna," *IEEE Trans. Antennas Propagat*., vol. AP-19 (September 1971): 692.
15. The Fourier-series analysis for the circular loop has a long history dating back to the work of H. C. Pocklington in 1897 on the closed loop. Recent treatments and additional references are in R. W. P. King and G. S. Smith, *Antennas in Matter: Fundamentals, Theory, and Applications* (Cambridge: The M.I.T. Press, 1981): 527–605; and R. W. P. King, "The Loop Antenna for Transmission and Reception," in R. E. Collin and F. J. Zucker (eds.), *Antenna Theory*, part I (New York: McGraw-Hill, 1969): 458–482. Tables of input admittance are in R. W. P. King, *Tables of Antenna Characteristics* (New York: Plenum Press, 1971): 151–160. The approach used by Japanese authors is described in N. Inagaki, T. Sekiguchi, and S. Ito, "A Theory of a Loop Antenna," *Electron. Commun. Japan*, vol. 53-B (March 1970): 62.
16. P. A. Kennedy, "Loop Antenna Measurements," *IRE Trans. Antennas Propagat*., vol. AP-4 (October 1956): 610.
17. G. Zhou and G. S. Smith, "An Accurate Theoretical Model for the Thin-Wire Circular Half-Loop Antenna," *IEEE Trans. Antennas Propagat*., vol. AP-39 (August 1991): 1167.

18. The near field of the circular loop with uniform current is discussed in P. L. Overfelt, "Near Fields of the Constant Current Thin Circular Loop Antenna of Arbitrary Radius," *IEEE Trans. Antennas Propagat*., vol. AP-44 (February 1996): 166, and the near field of the circular loop with a Fourier series for the current is treated by various methods in D. H. Werner, "An Exact Integration Procedure for the Vector Potentials of Thin Circular Loop Antennas," *IEEE Trans. Antennas Propagat*., vol. AP-44 (February 1996): 157 and (August 1996): 1199; L. W. Lin, M. S. Leong, S. Kooi, and T. S. Yeo, "Exact Solutions of Electromagnetic Fields in Both Near and Far Zones Radiated by Thin Circular-Loop Antennas: A General Representation," *IEEE Trans. Antennas Propagat*., vol. AP-45 (December 1997): 1741, vol. AP-49 (January 2001): 109, and (May 2001): 847; D. H. Werner, "Comments on Exact Solutions of Electromagnetic Fields in Both Near and Far Zones Radiated by Thin Circular-Loop Antennas: A General Representation," *IEEE Trans. Antennas Propagat*., vol. AP-49 (January 2001): 109; M. R. Abdul-Gaffoor, H. K. Smith., A. A. Kishk, and A. W. Glisson, "Comments on Exact Solutions of Electromagnetic Fields in Both Near and Far Zones Radiated by Thin Circular-Loop Antennas: A General Representation," *IEEE Trans. Antennas Propagat*., vol. AP-49 (May 2001): 845; and J. T. Conway, "New Exact Solution Procedure for the Near Fields of the General Thin Circular Loop Antenna," *IEEE Trans. Antennas Propagat*., vol. AP-53 (January 2005): 509.

19. The properties of a loop over an infinite image plane are obtained by using the theory of images and the analysis for an array of two loops; see, for example, K. Iizuka, R. W. P. King, and C. W. Harrison, Jr., "Self- and Mutual Admittances of Two Identical Circular Loop Antennas in a Conducting Medium and in Air," *IEEE Trans. Antennas Propagat*., vol. AP-14 (July 1966): 440.

20. S. Adachi and Y. Mushiake, "Directive Loop Antennas," *Res. Inst. Sci. Rep*., ser. B, vol. 9, no. 2, (Sendai, Japan: Tōhoku University, 1957): 105–112.

21. B. Rojarayanont and T. Sekiguchi, "One-Element Loop Antenna with Finite Reflector," *Electron. Commun. Japan*, vol. 59-B (May 1976): 68.

22. The coaxial array of driven loops is discussed in M. Kosugi, N. Inagaki, and T. Sekiguchi, "Design of an Array of Circular-Loop Antennas with Optimum Directivity," *Electron. Commun. Japan*, vol. 54-B (May 1971): 67; and S. Ito, M. Kosugi, N. Inagaki, and T. Sekiguchi, "Theory of a Multi-Element Loop Antenna," *Electron. Commun. Japan*, vol. 54-B (June 1971): 95.

23. S. Ito, N. Inagaki, and T. Sekiguchi, "Investigation of the Array of Circular-Loop Antennas," *IEEE Trans. Antennas Propagat*., vol. AP-19 (July 1971): 469.

24. H. W. Ehrenspeck and H. Poehler, "A New Method for Obtaining Maximum Gain from Yagi Antennas," *IRE Trans. Antennas Propagat*., vol. 7 (October 1959): 379.

25. M. Yamazawa, N. Inagaki, and T. Sekiguchi, "Excitation of Surface Wave on Circular-Loop Array," *IEEE Trans. Antennas Propagat*., vol. AP-19 (May 1971): 433.

26. The design of Yagi-Uda arrays of loops is discussed in J. E. Lindsay, Jr., "A Parasitic End-Fire Array of Circular Loop Elements," *IEEE Trans. Antennas Propagat*., vol. AP-15 (September 1967): 697; J. Appel-Hansen, "The Loop Antenna with Director Arrays of Loops and Rods," *IEEE Trans. Antennas Propagat*., vol. AP-20 (July 1972): 516; L. C. Shen and G. W. Raffoul, "Optimum Design of Yagi Array of Loops," *IEEE Trans. Antennas Propagat*., vol. AP-22 (November 1974): 829; N. Takata and T. Sekiguchi, "Array Antennas Consisting of Linear and Loop Elements," *Electron. Commun. Japan*, vol. 59-B (May 1976): 61; A. Shoamanesh and L. Shafai, "Properties of Coaxial Yagi Loop Arrays," *IEEE Trans. Antennas Propagat*., vol. AP-26 (July 1978): 547; and A. Shoamanesh and L. Shafai, "Design Data for Coaxial Yagi Array of Circular Loops," *IEEE Trans. Antennas Propagat*., vol. AP-27 (September 1979): 711.

27. G. P. Zhou and G. S. Smith, "The Multiturn Half-Loop Antenna," *IEEE Trans. Antennas Propagat*., vol. AP-42 (May 1994): 750.

28. The shielded loop is discussed in L. L. Libby, "Special Aspects of Balanced Shielded Loops," *IRE Proc*., vol. 34 (September 1946): 641; and R. W. P. King, "The Loop Antenna for Transmission and Reception," in R. E. Collin and F. J. Zucker (eds.), *Antenna Theory*, part I (New York: McGraw-Hill, 1969): 478–480. The shielded half loop as a current probe is treated in R. W. P. King and G. S. Smith, *Antennas in Matter: Fundamentals, Theory and Applications* (Cambridge: The M.I.T. Press, 1981): 770–787.

29. The loop with pulse excitation is analyzed in A. M. Abo-Zena and R. E. Beam, "Transient Radiation Field of a Circular Loop Antenna," *IEEE Trans. Antennas Propagat*., vol. AP-20 (May 1972): 380; G. Franceschetti and C. H. Papas, "Pulsed Antennas," *IEEE Trans. Antennas Propagat*., vol. AP-22 (September 1974): 651; K. J. Langenberg, "Pulsed Loop Antennas," *Appl. Phys*., vol. 10 (1976): 309; and K. J. Langenberg, "Transient Fields of Small Loop Antennas," *IEEE Trans. Antennas Propagat*., vol. AP-24 (March 1976): 236.

30. For more of the details for the discussion presented here, see G. S. Smith, *An Introduction to Classical Electromagnetic Radiation* (Cambridge, UK: Cambridge University Press, 1997): 567–575, and G. S. Smith, "Teaching Antenna Radiation from a Time-Domain Perspective," *Am. J. Phys*., vol. 69 (March 2001): 288.

31. K. P. Esselle and S. S. Stuchly, "Resistively Loaded Loop as a Pulse-Receiving Antenna," *IEEE Trans. Antennas Propagat*., vol. AP-38 (July 1990): 1123, and H. F. Li, Z. N. Chen, and L. W. Li, "Characterization of Resistive-Loaded Wire Loop in UWB (Impulse) Radio," *Microwave Opt. Technol. Lett*., vol. 43 (October 20, 2004): 151.

32. The analysis of elementary vertical and horizontal magnetic dipoles near a planar interface is discussed in A. Sommerfeld, *Partial Differential Equations in Physics* (New York: Academic Press, Inc., 1949): 237–279; A. Baños, Jr., *Dipole Radiation in the Presence of a Conducting Half-Space* (New York: Pergamon Press, 1966); and J. R. Wait, *Electromagnetic Waves in Stratified Media* (New York: Pergamon Press, 1970).

33. J. Ryu, H. F. Morrison, and S. H. Ward, "Electromagnetic Fields about a Loop Source of Current," *Geophysics*, vol. 35 (October 1970): 862; J. R. Wait and K. P. Spies, "Subsurface Electromagnetic Fields of a Circular Loop of Current Located above Ground," *IEEE Trans. Antennas Propagat*., vol. AP-20 (July 1972): 520; and J. R. Wait and K. P. Spies, "Low-Frequency Impedances of a Circular Loop over a Conducting Ground," *Electron. Lett*., vol. 9 (July 26, 1973): 346.

34. L. N. An and G. S. Smith, "The Horizontal Circular Loop Antenna near a Planar Interface," *Radio Sci*., vol. 17 (May-June 1982): 483.

35. Bare and insulated electrically small loop antennas in dissipative media are discussed in J. R. Wait, "Electromagnetic Fields of Sources in Lossy Media," in R. E. Collin and F. J. Zucker (eds.), *Antenna Theory*, part II (New York: McGraw-Hill, 1969): 438–514 and references therein. Bare and insulated loop antennas of general size are treated in R. W. P. King and G. S. Smith, *Antennas in Matter: Fundamentals, Theory and Applications* (Cambridge: The M.I.T. Press, 1981): 527–605; and L. N. An and G. S. Smith, "The Eccentrically Insulated Circular Loop Antenna," *Radio Sci*., vol. 15 (November–December 1980): 1067 and vol. 17 (May–June 1982): 737.

36. A. Lakhtakia, M. Iskander, C. H. Durney, and H. Massoudi, "Near-Field Absorption in Prolate Spheroidal Models of Humans Exposed to a Small Loop Antenna of Arbitrary Orientation," *IEEE Trans. Microwave Theory Tech*., vol. MTT-29 (June 1981): 588; W. T. Chen and H. R. Chuang, "Numerical Computation of Human Interaction with Arbitrary Oriented Superquadric Loop Antennas in Personal Communications," *IEEE Trans. Antennas Propagat*., vol. AP-46 (June 1998): 521; and W. T. Chen and H. R. Chuang, "Numerical Computation of the EM Coupling Between a Circular Loop Antenna and a Full-Scale Human-Body Model," *IEEE Trans. Microwave Theory Tech*., vol. MTT-46 (October 1998): 1516.